REVISTA MATÉRIA V.22 N.01

ISSN 1517-7076 artigo e11802, 2017

Evaluation of nickel and copper catalysts in biogas reforming for hydrogen production in SOFC

Leonardo Alves Silva[1], André Rosa Martins[1,2], Adriana Ballarini[3], Silvia Maina[3], Maria do Carmo Rangel[1]

[1]Grupo de Estudos em Cinética e Catálise, Instituto de Química, Universidade Federal da Bahia,Campus Universitário de Ondina, Federação, 40 170-280, Salvador, Bahia, Brazil. e-mail: mcarmov@ufba.br
[2]Instituto Federal da Bahia, Campus Porto Seguro, 45810-000, Porto Seguro, Bahia, Brazil.
[3]INCAPE "Ing José Parera"; Edificio CCT CONICET Santafe "Dr. Alberto Cassano"; Recolección Ruta Nac 168, km 0 - Paraje El Pozo - (3000) Santa Fe, Argentina.

ABSTRACT

The solid oxide fuel cells (SOFC) enable the efficient generation of clean energy, fitting the current requirements of the growing demand for electricity and for the environment preservation. When powered with biogas (from digesters of municipal wastes), the SOFCs also contribute to reduce the environmental impact of these wastes. The most suitable route to produce hydrogen inside SOFC from biogas is through dry reforming but the catalyst is easily deactivated by coke, because of the high amounts of carbon in the stream. A promising way to overcome this drawback is by adding a second metal to nickel-based catalysts. Aiming to obtain active, selective and stable catalysts for biogas dry reforming, solids based on nickel (15%) and copper (5%) supported on aluminum and magnesium oxide were studied in this work. Samples were prepared by impregnating the support with nickel and copper nitrate, followed by calcination at 500, 600 and 800 ^{o}C. It was noted that all solids were made of nickel oxide, nickel aluminate and magnesium aluminate but no copper compound was found. The specific surface areas did not changed with calcination temperature but the nickel oxide average particles size increased. The solids reducibility decreased with increasing temperature. All catalysts were active in methane dry reforming, leading to similar conversions but different selectivities to hydrogen and different activities in water gas shift reaction (WGSR). This behavior was assigned to different interactions between nickel and copper, at different calcination temperatures. All catalysts were active in WGSR, decreasing the hydrogen to carbon monoxide molar ratio and producing water. The catalyst calcined at 500 ^{o}C was the most promising one, leading to the highest hydrogen yield, besides the advantage of being produced at the lowest calcination temperature, requiring less energy in its preparation.

Keywords: fuel cell, biogas, dry reforming, hydrogen, nickel catalyst.

1. INTRODUCTION

In recent times, concerns on climate changes, as well as the growing need for energy, have promoted the development of renewable energy technologies for producing cleaner and more efficient energy [1, 2]. In addition, there is a need of generating electricity locally, avoiding the risks and costs related to energy distribution. The cleanest and most efficient way to generate electricity locally is by using fuel cells. These electrochemical devices directly convert the chemical energy stored in the fuel (gas or liquid) into electrical energy. Fuel cells are powered with a fuel containing hydrogen (which is electrochemically oxidized at an anode) and air (at the cathode) to produce electric power and an exhaust gas in one step, with high efficiency. This simplicity contrasts with the internal combustion engines in which chemical energy is first transformed into thermal energy by a combustion process and then transformed into mechanical energy and finally into electrical energy. The second step is the most inefficient since it is limited by the Carnot cycle [3, 4]. In addition, fuel cells do not produce significant amounts of pollutants, such as nitrogen oxides, especially when compared to internal combustion engines. These devices produce only water when powered with hydrogen and can be used for both stationary and portable power generation as well as in small and large scales, for several applications [3]. The versatility of fuel cells makes them suitable for uses in automobiles, computers, phones and other mobile equipment, besides in local power generation promoting the development of remote regions.

Among the several types of fuel cells, the solid oxide fuel cells (SOFC) are the most promising tech-

Corresponding Author: Maria do Carmo Rangel Received on: 23/05/2016 Accepted on: 14/12/2016

10.1590/S1517-707620170001.0134

nology to stationary applications such as power plants or combined heat and power generation [5-7]. These devices offer several advantages compared to other fuel cells, such as the potential to achieve higher base efficiencies and the ability to be adapted to combined heat and power applications with high efficiency, reaching up to 85%. Furthermore, they can be easily adapted to operate on different fuels, using low cost reformers [6]. Other advantages include wide range of applications, simple design, high efficiency, reliability, modularity, low levels of emissions of nitrogen oxides and sulfur and absence of noise usually associated with conventional power generation systems. SOFCs have a wide range of applications from the centralized megawatt-scale generation through to localized applications at greater 100 kW level for distribution to local domestic generation on the 10 kW scale [7].

Hydrogen is the fuel usually associated with fuel cells but it has low energy density, is volatile and flammable, being difficult to handle. In addition, there are difficulties in transportation and storage, besides the high cost. The generation of hydrogen inside the fuel cell (generation on board) through the fuel reforming is then a practical and viable option to overcome these drawbacks [3]. Therefore, the SOFC has been designed to operate with different fuels such as natural gas, alcohols, gasoline and others. Because of the high operating temperatures, these fuels can be reformed and these devices become more resistant to impurities, reducing the fuel processing and manufacturing costs [3,8].

The fuel may be reformed both externally or internally the cell. In external reforming, the fuel is converted into hydrogen and carbon dioxide, in a reformer. In this case, the endothermic reforming and the exothermic electrochemical reaction are performed in different units and there is no direct heat transfer between the operating units. For the internal reforming, the steam reforming and the oxidation reaction are carried out in the same compartment. The internal reforming may be performed by a direct or indirect way. In the indirect internal reforming, the process is physically separated from the electrochemical reaction by a wall, which allows the heat exchange both by conduction and radiation. On the other hand, in the direct internal reforming, the mixture of fuel and steam is powered directly to the anode compartment, where the fuel is reformed [9]. For all these arrangements, the electrochemical reaction may be carried out with a mixture of hydrogen and carbon monoxide, while avoiding steps of hydrogen purification, such as the water gas shift reaction [10] or the preferential oxidation of carbon monoxide [11], as required for proton exchange membrane fuel cells.

For the external or indirect internal reforming, the catalytic process is performed in an independent compartment from the anode one. This allows the catalysts to be selected based only on their catalytic properties, without attention to the electrochemical requirements. In any of these arrangements, the steam reforming (with water), dried (carbon dioxide), partial (with oxygen) or autothermal (water and oxygen) can be carried out, using methane (natural gas), ethanol , glycerin, biogas, biomass or other fuel containing hydrogen [12-20]. For all cases, the catalysts of steam reforming [12-16, 21, 22], dry [17, 23, 24] partial [20, 25, 26] or autothermal [18, 20], based on noble metals such as platinum, palladium, ruthenium, iridium and rhodium, besides nickel, cobalt and iron, can be used.

However, by considering local production of electricity using SOFC, biogas emerges as one of the most suitable and promising alternatives for sustainable energy source, since it does not contributes to carbon dioxide emissions by an annual growth cycle. Biogas is produced during anaerobic digestion processes of biomass from municipal waste or animal and agriculture waste and consists mainly of methane and carbon dioxide [27]. The inherent advantages of this fuel include low cost and availability in different locations, avoiding transportation, besides the possibility of generating local jobs. Despite these advantages and the widespread availability, this resource is still underutilized and only few technologies have been used in developing countries. However, biogas is widely used in USA for local power generation in wastewater treatment plants, although gas turbines were mostly used. Moreover, the efficiency of SOFC coupled to digesters for local generation of electricity has been demonstrated [28] and some systems have been already used in waste treatment plants in USA [29]. Therefore, several studies have been devoted to biogas-fed solid oxide fuel cells [27-36], aiming to improve these systems.

Due to the high carbon dioxide content in biogas, the most promising alternative is to perform dry reforming in biogas-fed solid oxide fuel cells. The dry methane reforming (Eq. 1) is an endothermic reaction, which has been attracted a growing interest from industrial and environmental perspective [36]. However, the high carbon content in biogas is a significant potential for coke formation on the catalyst, resulting in their deactivation [16, 23, 24, 28, 37]. The active and stable catalysts for biogas reforming are mostly noble metals, such as rhodium, palladium, iridium, platinum and ruthenium [38] besides inexpensive nickel which, however, is very active to coke deposition [39]. On the other hand, the addition of other metal, such as platinum, palladium, cobalt, molybdenum and copper can improve the catalytic performance of nickel [40, 41]. Aiming to obtain active and stable catalysts for producing hydrogen from biogas, catalysts based on nickel and copper supported on aluminum and magnesium oxides were studied in this work.

$$CH_{4(g)} + CO_{2(g)} \rightleftharpoons 2\,CO_{(g)} + 2\,H_{2(g)} \qquad \Delta H_{298K} = 247\ kJ.mol^{-1} \qquad (1)$$

2. MATERIALS AND METHODS

2.1 Catalysts preparation

The support (aluminum and magnesium oxide) was prepared at room temperature by precipitation technique, adding an aluminum nitrate solution (2.00 mol L^{-1}), a magnesium nitrate solution (1.00 mol L^{-1}) and an ammonium hydroxide solution (28% v/v) to a beaker with water, using a peristaltic pump (2.0 mL min^{-1}). During precipitation, the pH was kept around 9. After precipitation, the colloidal solution produced was maintained under stirring, for 24 h and centrifuged. The gel obtained was rinsed with an ammonium hydroxide solution (1% w/w) to remove nitrate ions and centrifuged again. The gel was dried at 120 °C, for 24 h and then heated (10 $^oC\ min^{-1}$) under air flow (60 mL min^{-1}) to 800 °C, being kept at this temperature for 2 h, to get the support (Sample MA800).

The catalysts were obtained by dispersing the support in a nickel nitrate (0.8519 mol L^{-1}) and copper nitrate solution (0.2623 mol L^{-1}), in order to obtain solids with 15% (w/w) of nickel and 5% (w/w) of copper. The solvent was evaporated under occasional stirring on a hot plate maintained at 60 °C and the solid was dried at 120 °C, for 24 h. It was then calcined at 500 °C for 2 h, generating the NMA500 sample. Other samples were prepared following the same procedure but calcining the solids at 600 ^oC (NMA600 sample) and 800 °C (NMA800 sample).

2.2 Catalysts characterization

The samples were characterized by X-ray diffraction (XRD), specific surface area (Sg) and porosity measurements and temperature programmed reduction (TPR). The metal sites of the catalysts were examined by the model reaction of cyclohexane dehydrogenation.

The X-ray diffraction profiles were recorded in a Siemens D5005 equipment, using CuKα radiation generated at 40 kV and 30 mA and a goniometer velocity of 2 degrees min^{-1}, in the range of 2θ= 10 to 80 degrees. The samples were analyzed at room temperature and without prior treatment. The crystalline phases were identified by comparing the data obtained with the files of the International Centre for Diffraction Data files (ICDD). For specific surface area and porosity measurements, the adsorption and desorption of nitrogen were performed on a Micromeritics ASAP 2020 equipment. Prior the analysis, the sample (0.20 g) was heated (10 °C min^{-1}) under vacuum up to 250 °C and kept at this temperature for 4 h for the removal of humidity from the solids. During the analysis, the sample was exposed to pulses of nitrogen until a maximum increase of pressure of 925 mmHg. The temperature programmed reduction experiments were performed on a 2900 Analyzer Micromeritics equipment. The sample (around 0.200 g) was heated (10 °C min^{-1}) under nitrogen flow (60 mL min^{-1}) up to 160 °C and kept at this temperature for 30 min to remove water and impurities from the surface. The sample was then cooled to room temperature and heated (10 °C min^{-1}) under flowing (60 mL min^{-1}) of a mixture of 5% H_2/N_2 up to 1000 °C. During the experiments, the hydrogen consumption was monitored by a thermal conductivity detector (TCD).

The experiments of cyclohexane dehydrogenation, a model reaction for metallic sites, were performed in equipment built in our laboratory, working at 300 ^oC and 1 atm. The sample (0.100 g) was loaded in a quartz reactor, purged under nitrogen flow and then reduced under hydrogen flow (60 mL min^{-1}) at 750 ^oC, for 2:30 h. Cyclohexane was then fed (0.0067 mL min^{-1}) to the reactor. The effluent was analyzed each 5 min for 1 h, by on line GC-8A model Shimadzu chromatograph equipped with a flame ionization detector (FID) and a packed column.

2.3 Catalysts evaluation

The dry reforming of methane was carried out in a continuous flow reactor, kept at 700 °C and fed with 20 ml^{-1} of a mixture of methane to carbon dioxide molar of 1. Before reaction, the catalyst (0.2) was reduced in situ under hydrogen flow at 700 °C, for 2:30 h. Each run took 300 min., The reaction products were analyzed on line by a Star 3400 CX Varian gas chromatograph equipped with a TCD and 1006 Carboxem3 column.

3. RESULTS AND DISCUSSION

Figure 1 shows the X-ray diffraction of the support and of the catalysts obtained at different temperatures. It can be noted that the support (MA800 sample) showed peaks typical of magnesium aluminate spinel (ICSD

21-1152) and no peak related to alumina or magnesium oxide (periclase) was noted. This finding is agreement with previous works [42-44], which claim that at temperatures as high as 800 °C, the crystalline phase of magnesium aluminate spinel ($MgAl_2O_4$) is the only compound produced in the MgO-Al_2O_3 system, which is more thermodynamically stable than alumina.

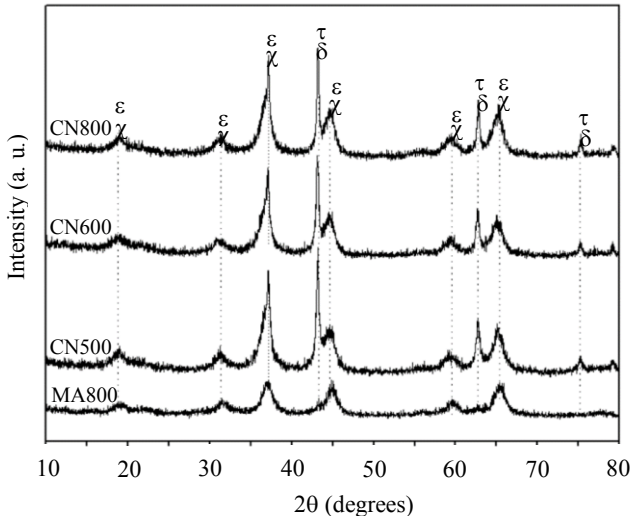

Figure 1: X-ray diffractograms for the support and for the catalysts calcined at different temperatures. Identification of phases: (χ) $MgAl_2O_4$; (ε) $NiAl_2O_4$; (δ) NiO and (τ) MgO.

After nickel addition, the peaks became narrower and more intense, indicating the increase of the crystalline domains and/or nickel aluminate formation (ICSD 77-1877). The peaks in 2θ= 43, 62 and 75 degrees indicate the segregation of nickel oxide (ICSD 73-1523). The periclase phase of magnesium oxide (ICSD 75-1525) could not be identified because the position of the peaks coincides with those of nickel oxide. Furthermore, no peak related to copper oxide was found, suggesting that copper species are well dispersed on the support. The increase of the calcination temperature did not produce any other phase. However, one can see an increase of peak intensity with temperature, especially in the case of the sample calcined at 800 °C, indicating an increase of crystals size. Table 1 shows the average crystals diameter of nickel oxide for the catalysts, calculated from the X-ray diffractograms using the Scherrer equation by the (202) plane. As we can see, no significant difference was found for the samples calcined at 500 and 600 °C, but an increase of the average crystal size was noted for the sample calcined at 800 °C. The specific surface areas of the samples are also shown in Table 1. It can be noted that the addition of nickel and copper to the support (MA800 sample) caused a decrease in the specific surface area of the solid. On the other hand, the catalysts calcined at different temperatures showed similar values (close to 100 $m^2\ g^{-1}$), indicating that the catalysts were stable in the range of 500-800 °C.

Table 1: Average crystals diameter of nickel oxide and specific surface areas of the support and of the catalysts calcined at different temperatures.

SAMPLE	AVERAGE CRYSTALS DIAMETER (NICKEL OXIDE) (nm)	SPECIFIC SURFACE AREAS ($m^2\ g^{-1}$)
MA800	--	160
CN500	36	103
CN600	33	97
CN800	47	117

Figure 2 shows the curves for adsorption/desorption of nitrogen as a function of relative pressure. For all cases, isotherms with intermediate profiles between types II and IV were obtained, which are typical of macroporous solids. In addition, a loop of H4 hysteresis-type can be noted, indicating the existence of interparticle mesopores [45]. The temperature increase did not change significantly the isotherms profile, indi-

cating that the textural properties of the solids were not affected by calcination temperature.

On the other hand, the calcination temperature significantly changed the reduction profiles of the catalysts, as shown in Figure 3. The catalyst calcined at 500 °C showed two peaks at low temperatures (324 and 422 °C), which can be assigned to the reduction of bigger particles of nickel oxide in weak interaction with the support, in accordance with previous work [39]. The lowest-temperature peak can also be associated to the reduction of copper species interacting with alumina [46, 47]. These peaks were less intense for the catalyst calcined at 600 °C and disappeared in the case of the sample calcined at 800 °C, indicating an increase of interaction of the metals with the support, rendering the segregation of nickel oxide. A broad peak at high temperatures, centered at 665 °C, was also noted for the solid calcined at 500 °C, indicating the reduction of nickel species in different interactions with the support [46]. According to several works [26, 39, 45, 48], various processes may occur at this temperature range such as the reduction of small nickel oxide particles in strong interaction with the support, nickel oxide containing aluminum species in the lattice or nickel aluminate. It can be also noted that the high temperature peak was shifted to higher temperatures as the calcination temperature was increased, indicating an increase of interaction of nickel with the support, as found in a previous work [49]. The amount of hydrogen consumed during the TPR experiments are shown in Table 2, as well as the degree of reduction of the solid, calculated from this consumption. We can see that the degree of reduction decreased as the calcination temperature increased, a fact that can be related to the increase of the strength of interaction between nickel and the support, leading to the production of nickel aluminate, which is difficult to be reduced [39].

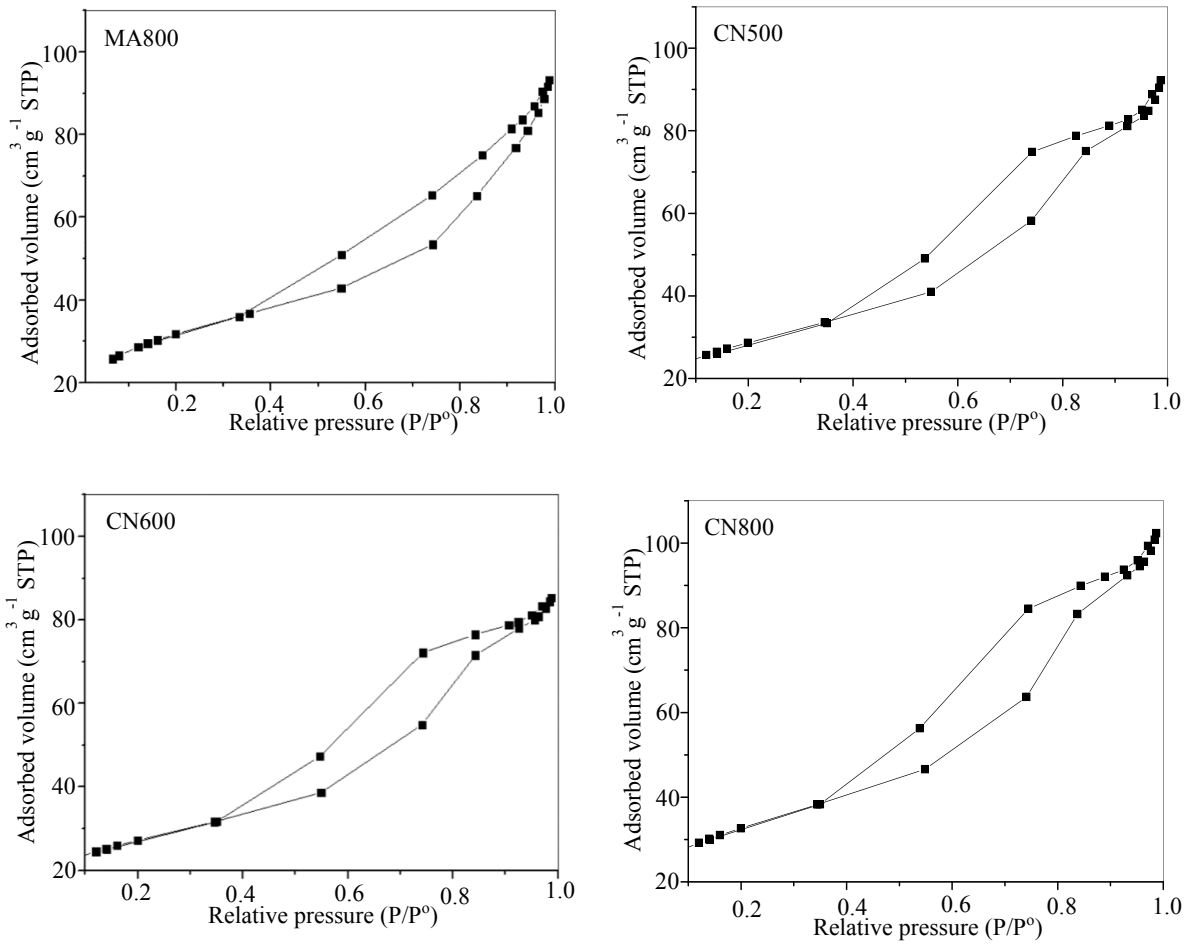

Figure 2: Nitrogen adsorption/desorption isotherms for the support (MA800) and for the catalysts calcined at 500 (CN500), 600 (CN600) and 800 °C (CN800).

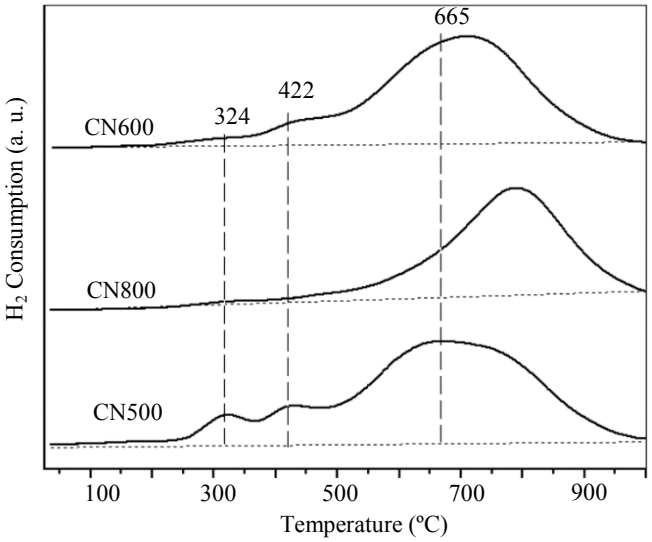

Figure 3: TPR profiles for the catalysts calcined at different temperatures.

Table 2: Expected and obtained hydrogen consumptions during the TPR experiments and reduction degree of the catalysts calcined at different temperatures and values of conversion during cyclohexane dehydrogenation.

SAMPLES	EXPECTED HYDROGEN CONSUMPTION (mmol)	OBTAINED HYDROGEN CONSUMPTION (mmol)	REDUCTION DEGREE (%)	CYCLOHEXANE CONVERSION (%)
CN500	0.38093	0.30660	80	8.43
CN600	0.38359	2.5721	67	8.89
CN800	0.37186	2.2188	60	5.84

Table 2 also shows the values of conversion during cyclohexane dehydrogenation, a reaction which does not demand a special metallic structure or particle size, being a non-demanding reaction, as pointed out by Boudart and coworkers [50]. Therefore, the conversion values depend only on the number of exposed metal atoms [51] and then can be related to metal dispersion. From Table 2, it can be also observed that the catalysts calcined at 500 and 600 ^{o}C led to similar values of cyclohexane conversion, indicating that they have similar amounts of metal atoms exposed on the surface. On the other hand, the catalyst calcined at 800 ^{o}C led to the lowest conversion, indicating that it has the lowest dispersion and then the bigger nickel particles, in agreement with the X-ray diffraction results.

All catalysts were active in dry reforming of methane (Equation 1) and were stable during reaction, as shown in Figure 4. One can note that the values of methane conversion were slightly affected by the calcination temperature, the catalysts leading to similar values regardless the calcination temperature. The same tendency was noted for carbon dioxide conversions. However, the carbon dioxide conversions were always higher than the methane conversions, indicating to the occurrence of reverse water gas shift reaction (WGSR), which also consumes carbon dioxide (Equation 2) [49], as found previously [24]. As pointed out early [46], both copper and nickel are active in WGSR (Equação 2).

$$CO_{2(g)} + H_{2(g)} \rightleftharpoons CO_{(g)} + H_2O_{(g)} \qquad \Delta H_{298K} = 41 \text{ kJ.mol}^{-1} \qquad (2)$$

The catalyst calcined at 500 ^{o}C led to the highest value of methane conversion and showed the highest hydrogen selectivity. This can be related to its highest reduction degree of this catalyst, generation more active sites. However, the catalysts calcined at 600 and 800 ^{o}C showed similar hydrogen selectivities and the

sample calcined at 600 °C led to the lowest methane conversion in spite of being the second more reducible catalyst, besides having the smallest average nickel oxide particle size. This finding suggested that different interactions occurred in this solid, decreasing the ability of nickel in breaking the C-H bonds in methane. It has been demonstrated [52] that the addition of copper to nickel can decrease the activity of nickel catalysts in methane decomposition. Moreover, it has been reported [53] that copper, with a full-filled 3d orbital, is not active in methane decomposition. However, copper is relatively rich in d electrons and then it can exert electronic effects on nickel atoms, by increasing their activity for breaking the C-H bonds [52]. Therefore, the effect of copper on nickel activity largely depends on the interaction between these metals, which in turn depends on the preparation method, including the calcination temperature. In our work, it is possible that above 500 °C, the higher amounts of nickel atoms have occluded copper atoms resulting in no effect of copper on the breakage of C-H bonds and then on methane reforming. On the other hand, for the catalyst calcined at 800 °C, this effect was compensated by the formation of nickel aluminate, which is known to generate very active sites for methane reforming [39]. As found by TPR, the reduction profile of this sample is typical of nickel aluminate [39, 49]. These catalysts produced the highest amount of water, indicating that they are the most active in the reverse WGSR, probably due to nickel atoms [54]. The hydrogen to carbon monoxide molar ratios were lower than 1.0 for all catalysts, as shown in Table 3. This is related to the reverse WGSR, which consumes hydrogen and produces carbon monoxide. Is can also be noted that the catalyst calcined at 500 °C led to the highest hydrogen yield, being the most suitable to methane dry reforming.

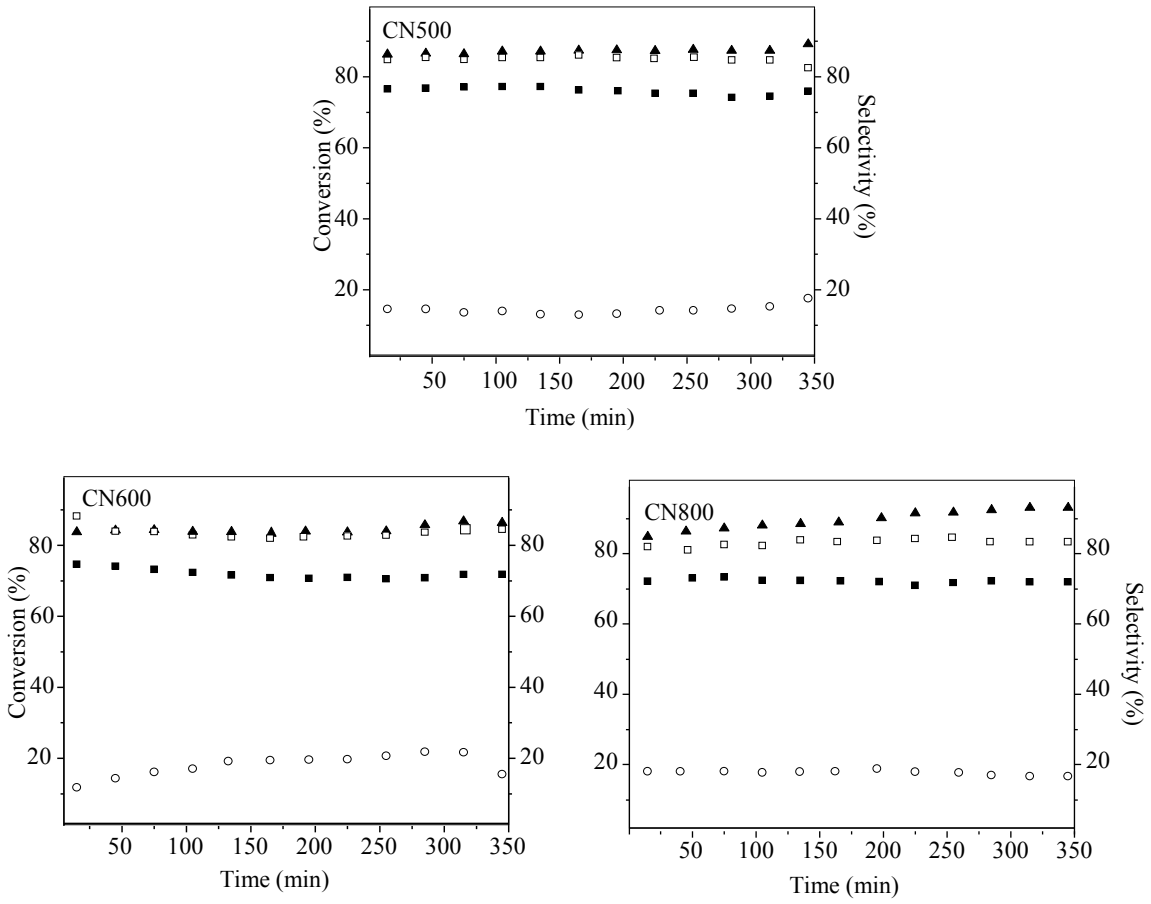

Figure 4: Conversion of the reactants and selectivity of the catalysts calcined at different temperatures as a function of time during methane dry reforming. (■) methane conversion; (▲) carbon dioxide conversion; (□) hydrogen selectivity and (○) water.

Table 3: Hydrogen to carbon monoxide molar ratio and hydrogen yield obtained over the catalysts calcined at different temperatures.

SAMPLES	HYDROGEN/CARBON MONOXIDE	HYDROGEN YIELD (%)
CN500	0.8	68
CN600	0.7	61
CN800	0.7	64

4. CONCLUSIONS

Catalysts based on nickel (15%) and copper (5%) supported on magnesium and aluminum oxide were obtained by calcining the solids at 500, 600 and 800 ^{o}C, after impregnating the support with nickel and copper nitrate. All catalysts were made of nickel oxide, nickel aluminate and magnesium aluminate, copper compounds not being identified, regardless the calcination temperature. However, the catalysts showed different reduction profiles, the reducibility decreasing with increasing of calcination temperature. The catalysts showed similar specific surface areas but different nickel oxide average particles size, which increased with calcination temperature. The catalysts also showed different amounts of exposed metal atoms on the surface, evaluated by cyclohexane dehydrogenation. All catalysts were active in methane dry reforming, leading to similar conversions. The catalyst calcined at 500 °C showed the highest activity and hydrogen selectivity, followed by the solid calcined at 800 ^{o}C, the sample calcined at 600 ^{o}C being the least active and selective.

These findings were assigned to different interactions between nickel and copper, at different calcinations temperatures, leading to different amounts of nickel exposed on the surface and to nickel species with different catalytic activity. All catalysts were active to reverse water gas shift reaction, decreasing the hydrogen to carbon monoxide molar ratio and producing water. The catalyst calcined at 500 ^{o}C was the most active in methane dry reforming and selective to hydrogen and the least active in reverse water gas shift reaction.

Therefore, it is the most promising catalysts among the studied samples, with the advantages of being produced at the lowest calcination temperature requiring less energy in the preparation.

5. ACKNOWLEDGEMENTS

LAS and ARM thank the Permanecer programme/UFBA and to CNPq, respectively, for the scholarships. The authors thank CNPq and PETROBRAS for the financial support.

6. BIBLIOGRAPHY

[1] BILGEN, S., “Structure and environmental impact of global energy consumption”, *Renewable and Sustainable Energy Reviews*, v. 38, pp. 890–902, Jul. 2014.

[2] RANGEL, M. C., CARVALHO, M. F. A., “Impact of automotive catalysts in the control of air quality”, *Química Nova*, v. 26, n. 2, pp. 265–277, Mar. 2003.

[3] ATIKINSON, A., BARNETT, S., GORTE, R. J., *et al*., “Advanced anodes for high-temperature fuel cells”, *Nature Materials*, v.3, pp. 17-27, Jan. 2004.

[4] SÁNCHEZ, D., CHACARTEGUI, R., MUÑOZ, A., *et al*., “On the effect of methane internal reforming modelling in solid state fuel cells”, *International Journal of Hydrogen Energy*, v. 33, pp. 1834-1844, Mar. 2008.

[5] CORDEIRO, R. C., TRINDADE, G. S., MAGALHÃES, R. N. S. H., *et al.*, “Nanostructured Ceramic Suspensions for Electrodes and the Brazilian SOFC Network ‘REDE PaCOS”, In: Bansal, N. P., Wereszczak, A., Lara-Curzio, E. (eds), *Advances in Solid Oxide Fuel Cells II: Ceramic Engineering and Science Proceedings,* v. 27, n. 5, pp. 138–152, chapter 14, Wiley Online Library, 2007.

[6] POTTER, E. N., “The Emergency of viable solid oxide fuel cell technology”, *Fuel Cells Bulletin*, v. 3, pp. 8-11, Nov. 2000.

[7] SINGHAL, S., “Advances in solid oxide fuel cell technology”, *Solid State Ionics*, v. 135, pp. 305–313, Nov. 2000.

[8] AGNEW, G.D., BERNARDI, D., COLLINS, R. D., CUNNINGHAM, R.H., “An Internal reformer for a pressurised SOFC system”, *Journal of Power Sources*, v. 157, pp. 832-836, Jan. 2006.

[9] CHOUDHURY, A., CHANDRA, H., ARORA, A., "Application of solid oxide fuel cell technology for power generation-A review", *Renewable and Sustainable Energy Reviews*, v. 20, pp. 430–442, Jan. 2013.

[10] PEREIRA, A. L. C., SANTOS, N. A., FERREIRA, M. L. O., *et al*., "Effect of Cobalt on the Activity of Iron-based Catalysts in Water Gas Shift Reaction", *Studies in Surface Science and Catalysis*, v.167, pp.225 - 230, Mai. 2007.

[11] MOURA, J. S., FONSECA, J. S. L, BION, N., *et al*., "Effect of lanthanum on the properties of copper, cerium and zirconium catalysts for preferential oxidation of carbon monoxide", *Catalysis Today*, v.228, pp. 40-50, Jun. 2014.

[12] ZHANG, Y., WANG, W., WANG, Z., *et al*., "Steam reforming of methane over Ni/SiO_2 catalyst with enhanced coke resistance at low steam to methane ratio", *Catalysis Today*, v. 256, pp. 130–136, Fev. 2015.

[13] SILVA NETO, A. V., SARTORATTO, P. P. C., RANGEL, M. C., "Preparation of Ni/SiO_2, Ni/SiO_2-CaO and Ni/SiO_2-MgO Catalysts for Methane Steam Reforming", *Studies in Surface Science and Catalysis*, v.167, pp.475-480, May 2007.

[14] OSORIO-VARGAS, P., FLORES-GONZÁLEZ, N. A., NAVARRO, R. M., *et al*., "Improved stability of Ni/Al_2O_3 catalysts by effect of promoters (La_2O_3, CeO_2) for ethanol steam-reforming reaction", *Catalysis Today*, v. 259, pp. 27–38, Jun. 2015.

[15] MOURA, J. S., SOUZA, M. O. G., BELLIDO, J. D. A., *et al*., "Ethanol steam reforming over rhodium and cobalt-based catalysts: Effect of the support", *International Journal of Hydrogen Energy*, v. 37, pp. 3213-3224, Feb. 2012.

[16] MARTÍNEZ, L.M. T., ARAQUE, M., CENTENO, M. A., *et al*., "Role of ruthenium on the catalytic properties of CeZr and CeZrCo mixed oxides for glycerol steam reforming reaction toward H_2 production", *Catalysis Today*, v. 242, pp. 80–90, Mar 2015.

[17] FERNANDES JUNIOR, L. C. P., MIGUEL, S., FIERRO, J. L. G., *et al*., "Evaluation of Pd/La_2O_3 for Dry Reforming of Methane", *Studies in Surface Science and Catalysis*, v.167, pp.499-504, May 2007.

[18] ZHAO, H., GUO, L., ZOU, X., "Chemical-looping auto-thermal reforming of biomass using Cu-based oxygen carrier", *Applied Energy*, v. 157, pp. 408-415, Nov. 2015.

[19] GIL, M. V., FERMOSO, J., PEVIDA, C., *et al*., "Production of fuel-cell grade H2 by sorption enhanced steam reforming of acetic acid as a model compound of biomass-derived bio-oil", *Applied Catalysis B: Environmental*, v. 184, pp. 64-76, May 2016.

[20] XIE, J., SUN, X., BARRETT, L., *et al*., "Autothermal reforming and partial oxidation of n-hexadecane via Pt/Ni bimetallic catalysts on ceria-based supports", *International Journal of Hydrogen Energy*, v. 40, pp. 8510-8521, July 2015.

[21] MOURA, J. S., RANGEL, M. C., SOUZA, M. O. G., "Effect of magnesium on the properties of nickel and lanthanum-based catalysts in steam reforming", *Fuel*, v.87, pp. 3627-3630, Dec. 2008.

[22] CARVALHO, L. S., MARTINS, A. R., REYES, P., *et al*., "Preparation and characterization of $Ru/MgO\text{-}Al_2O_3$ catalysts for methane steam reforming", *Catalysis Today*, v.142, pp. 52-60, Apr. 2009.

[23] WANG, F., XU, L., ZHANG, J., *et al*., "Tuning the metal-support interaction in catalysts for highly efficient methane dry reforming reaction", *Applied Catalysis B: Environmental*, v. 180, pp. 511-520, Jan. 2016.

[24] ARAÚJO, G. C., LIMA, S. M., ASSAF, J. M., *et al*., "Catalytic evaluation of perovskite-type oxide $LaNi_{1-x}Ru_xO_3$ in methane dry reforming", *Catalysis Today*, v.133-35, pp.129-135, Apr-Jun, 2008.

[25] ARAÚJO, G. C., LIMA, S., RANGEL, M. C., *et al*., "Characterization of Precursors and Reactivity of $LaNi_{1-x}Co_xO_3$ for the Partial Oxidation of Methane", *Catalysis Today*, v.107-08, pp.906-912, Oct 2005.

[26] BERROCAL, G. P., SILVA, A. L. M., ASSAF, J. M., *et al*., "Novel supports for nickel-based catalysts for the partial oxidation of methane", *Catalysis Today*, v.149, pp. 240-247, Jan. 2010.

[27] MURADOV, N., SMITH, F., T-RAISSI, A., "Hydrogen production by catalytic processing of renewable methane-rich gases", *International Journal of Hydrogen Energy*, v. 33, pp. 2023–2035, Apr. 2008.

[28] SHIRATORI, Y., OSHIMA, T., SASAKI, K., "Feasibility of direct-biogas SOFC", *International Journal of Hydrogen Energy*, v. 33, pp. 6316-6321, Nov. 2008.

[29] MURPHY, D. M., RICHARDS, A. E., COLCLASURE, A., *et al*., "Biogas fuel reforming for solid oxide fuel cells", *Journal of Renewable and Sustainable Energy*, v. 4, pp. 023106, Mar 2012.

[30] SHIRATORI, Y., IJICHI, T., OSHIMA, T., *et al*., "Internal reforming SOFC running on biogas", *International Journal of Hydrogen Energy*, v. 35, pp. 7905–7912, Aug. 2010.

[31] TAKAHASHI, Y., SHIRATORI, Y., FURUTA, S., *et al*., "Thermo-mechanical reliability and catalytic activity of Ni–Zirconia anode supports in internal reforming SOFC running on biogas", *Solid State Ionics*, v. 225, pp. 113–117, Oct. 2012.

[32] MANENTI, F., PELOSATO, R., VALLEVI, P., *et al*, "Biogas-fed solid oxide fuel cell (SOFC) coupled to tri-reforming process: Modelling and simulation", *International Journal of Hydrogen Energy*, v. 40, 14640-14650, Nov. 2015.

[33] ARESPACOCHAGA, N., VALDERRAMA, C., PEREGRINA, C., *et al*., "Evaluation of a pilot-scale sewage biogas powered 2.8 kWe Solid Oxide Fuel Cell: Assessment of heat-to-power ratio and influence of oxygen content", *Journal of Power Sources*, v. 300, pp. 325-335, Dec. 2015.

[34] STEELE, B. C. H., HEINZEL, A., "Materials for fuel-cells technologies", *Nature*, v. 414, pp 345-352, Nov. 2001.

[35] ANDRADE, M. L., ALMEIDA, L., RANGEL, M. C., *et al*., "Ni-Catalysts Supported on Gd-Doped Ceria for Solid Oxide Fuel Cells in Methane Steam Reforming", *Chemical Engineering & Technology*, v. 37, pp. 343–348, Feb. 2014.

[36] VAN HERLE, J., MEMBREZ, Y., BUCHELI, O., "Biogas as a fuel source for SOFC co-generators", *Journal of Power Sources*, v. 127, pp. 300–312, Mar. 2004.

[37] SHIRATORI, Y., SASAKI, K., "NiO–ScSZ and $Ni_{0.9}$Mg0.1O–ScSZ-based anodes under internal dry reforming of simulated biogas mixtures", *Journal of Power Sources*, v. 180, pp. 738–741, Jun. 2208.

[38] PAKHARE, D., SPIVEY, J., "A review of dry (CO_2) reforming of methane over noble metal catalysts", *Chemical Society Reviews*, v. 43, pp. 7813-7837, Feb. 2014.

[39] LIMA, S. P. DE, VICENTINI, V., FIERRO, J. L. G., *et al*., "Effect of aluminum on the properties of lanthana-supported nickel catalysts", *Catalysis Today*, v.133-35, pp. 925-930, Apr-Jun. 2008.

[40] AWADALLAH, A. E., ABOUL-ENEIN, A. A., ABOUL-GHEIT, A. K., "Various nickel doping in commercial Ni–Mo/Al_2O3 as catalysts for natural gas decomposition to COx-free hydrogen production", *Renewable Energy*, v. 57, pp. 671–678, Sep. 2013.

[41] HERMES, N.A., LANSARIN, M.A., PEREZ-LOPEZ, O.W., "Catalytic Decomposition of Methane Over M–Co–Al Catalysts (M= Mg, Ni, Zn, Cu)", *Catalysis Letters*, v. 141, pp. 1018–1025, May 2011.

[42] GADALLA, A. M. BOWER, B., "The role of catalyst support on the activity of nickel for reforming methane with CO_2", *Chemical Engineering Science*, v. 43, n.11, pp. 3049-3062, 1988.

[43] VOLLWEILER, L., JOST, H., HAUSNER, H., ", *Key Engineering Materials*, v.132-136, pp. 1814-1817, Apr.1997.

[44] REVERÓN, H., GUTIÉRREZ-CAMPOS, D., RODRÍGUEZ, R. M., *et al*., "Chemical synthesis and thermal evolution of $MgAl_2O_4$ spinel precursor prepared from industrial gibbsite and magnesia powder", *Materials Letters*, v. 56, pp. 97-101, n.1-2, Sep.2002.

[45] ROUQUEROL, F., ROUQUEROL, J., SING, K., Adsorption by Powders and Porous Solids: Principles, Methodology and Applications, London, Academic Press, 1998.

[46] FUENTES, E. M. COSTA, A. F., SILVA, T. F., *et al*., "A comparison between copper and nickel-based catalysts obtained from hydrotalcite-like precursors for WGSR", *Catalysis Today*, v.171, pp. 290-296, Aug. 2011.

[47] MOURA, J. S., SILVA, L. A., RANGEL, M. C., *et al*., "Synthesis and characterization of pervskite in $LaNi_{1-x}Cu_xO_3$ in hydrogen purificarton through PaCOS", *Revista Matéria*, v. 15, n. 3, pp. 472–479, 2010.

[48] CAVANI, F. TRIFIRO, F., VACCARI, A., "Hydrotalcite-type anionic clays: Preparation, properties and applications", *Catalysis Today*, v. 11, n. 2, pp. 173-301, Dec. 1991.

[49] METTE, K., KÜHL, S., TARASOV, A., *et al*., "Redox dynamics of Ni catalysts in CO_2 reforming of methane", *Catalysis Today*, v. 242, pp. 101-110, Mar. 2015.

[50] BOUDART, M., ALDAG, A., BENSON, J. E., *et al*., "On the Specific Activity of Platinum Catalysts", *Journal of Catalysis*, v. 6, pp. 92–99, Aug.1966.

[51] RANGEL, M. C., PARERA, J. M., CARVALHO, L. S., *et al*., "n-Octane Reforming over Alumina Supported Pt, Pt-Sn and Pt-W Catalysts", *Catalysis Letters*, v. 64, p.171-178, 2000.

[52] SHEN, Y., LUA, A. C., "Synthesis of Ni and Ni–Cu supported on carbon nanotubes forhydrogen and carbon production by catalytic decompositionof methane", *Applied Catalyis B: Environmental*, v. 164, pp. 164, 61–69, Mar. 2015.

[53] RODRIGUEZ, N.M., KIM, M. S., BAKER, R. T.K. "Deactivation of copper-nickel catalysts due to changes in surface composition", *Journal of Catalysis*, v. 140, n. 1, pp. 16–29, Mar. 1993.

[54] FUENTES, E. M., AIRES, F. C. S., PRAKASH, J. S., *et al*., "The effect of metal content on nickel-based catalysts obtained from hydrotalcites for WGSR in one step", *International Journal of Hydrogen Energy*, v.39, pp. 815-828, Jan. 2014.